Chapter 2

Sub-Barrier Fusion

What is fusion? The term fusion is sometimes used quite generally to describe any process in which the projectile and target interact strongly. To be more specific, fusion means the complete amalgamation of the target and projectile (full momentum transfer) to form a compound system which attains complete equilibrium in all degrees of freedom. The only memory the system retains of its formation is through conserved quantities such as mass, charge, energy, angular momentum and isospin. This is the Neils Bohr compound nucleus. However, one needs to verify experimentally that the conditions of the definition have been satisfied. The meaning of fusion becomes valid only if the decay of the compound system is consistent with the predictions of models for the decay of equilibrated systems. The Hauser-Feshbach (statistical) theory of the formation and decay of the compound nucleus is generally used for this purpose. Thus we identify fusion with the formation of a compound nucleus whose decay is governed by statistical considerations.

2.1 The Compound Nucleus Formation and Decay

The term 'compound nucleus' describes a nuclear system composed of the nucleons from the two collision partners which is not defined as an eigenstate of the total Hamiltonian of the system, but as a mixture of transitory configurations. Generally

these states have a very complicated structure and are assumed to be in statistical equilibrium with each other. The lifetime of a compound nucleus lies between 10^{-19}s and 10^{-16}s. The compound nucleus is highly excited and has a temperature. It also carries an angular momentum equal to the sum of the angular momentum of the relative motion in the entrance channel and the spins of the initial collision partners. The excitation energy and the angular momentum of the compound nucleus are eventually released via a decay process to the ground state. For compound nuclei at energies corresponding to incident laboratory energies $E < 10$ MeV per nucleon of the projectile, two main decay schemes can be identified:

- **Evaporation**, *i.e.* emission of light particles like neutrons, protons and α-particles. There remains a bound residual nucleus called *evaporation residue* of a slightly lower mass than the compound nucleus. The particle evaporation process is generally accompanied by γ emission.

- **Fission**, where the compound nucleus splits up into two halves of more or less equal size. This process is accompanied by evaporation of light particles out of the fissioning nucleus, and also the fission fragments will decay further by evaporation. These emitted particles are called 'pre scission' and 'post scission' particles respectively.

For lighter systems evaporation predominates. The rate of production of evaporation residues is then a measure of the fusion cross section. For medium heavy systems evaporation competes with the fission process. For heavy systems fission is the predominant mode of decay. In general it is the sum of the measured cross sections for these two main modes of decay which yields the magnitude of the fusion cross section.

The evaporation of particles from the compound nucleus depends in general on the angular momentum distribution of the initial compound nucleus. Fig. 2.1 shows the possible paths of de-excitation for a medium heavy compound nucleus

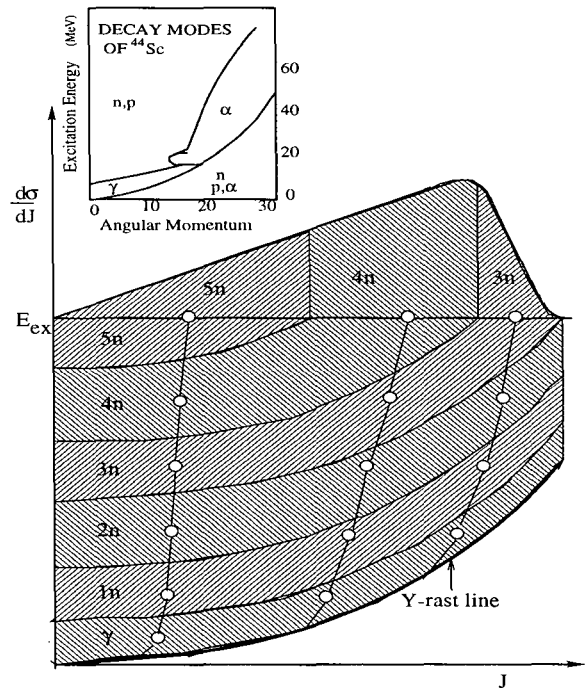

Figure 2.1: Decay of a highly excited heavy compound nucleus (A≈ 150) by neutron and gamma emission. Top: angular momentum distribution of the primary compound nucleus; bottom: typical decay path in the $E_{ex} - J$ plane. In the inset is shown the dominant decay mode for a light compound nucleus (A = 44).

($A \approx 150$) in the energy *vs* angular momentum plane. The accessible part of that plane is bounded by the 'yrast line' which connects the states of lowest energy for each angular momentum J. Here it is assumed that neutron emission is the dominant mode of particle decay. Each step of neutron emission removes a certain amount of excitation energy, equal to the sum of the neutron separation energy and the kinetic energy of the emitted neutron. The associated change in angular momentum is relatively small due to the small mass and average energy of the evaporated neutrons. Finally when the excitation energy above the yrast line is almost equal to or less than the neutron separation energy, neutron emission is strongly inhibited and gamma emission takes over. The remaining excitation energy and angular momentum are then dissipated by a series of electromagnetic transitions which proceed initially as

a statistical cascade towards the yrast line, and eventually pass through a sequence of yrast states to the ground state. From the figure one can see that the number of emitted neutrons decreases with increasing angular momentum. It should also be noted that each decay passes through a sequence of neighbouring isotopes which cannot be distinguished.

In the above discussion it was assumed that neutron emission is the main decay mode which is justified for compound nucleus of intermediate mass (A = 100 - 180) and moderate angular momentum (not too close to the yrast line) because of the absence of the Coulomb barrier. Charged particles, like protons or α-particles must be emitted with higher kinetic energies to overcome the respective Coulomb barriers. Consequently the final nuclei are produced at lower excitation energy where the density of levels and hence the number of open decay channels is strongly reduced. For lighter compound nuclei ($A < 100$), where the Coulomb barriers are lower, charged particle emission is favoured especially since the separation energies for charged particles are often smaller than those for neutrons. The inset in Fig. 2.1 shows the decay modes for a light compound nucleus (A = 44). Similarly for heavy compound nuclei ($A > 200$) the fission barrier (at zero angular momentum) becomes comparable with typical nucleon separation energies, and α emission is favoured by Q values. Therefore in general, charged particle emission is favourable both for light and for very heavy compound nuclei.

In principle, compound nucleus formation can be observed by detecting any of the following decay products: heavy evaporation residues, light evaporation products (mainly α-particles, protons, and neutrons), gamma rays emitted in the decay of bound excited states of the residual nuclei, and finally delayed beta or gamma radiation from the decay of the radioactive products. The gamma technique has been especially effective in the study of fusion of light nuclei. In very heavy compound systems (trans lead), decay is predominantly by fission, and fusion cross sections are obtained by measuring the fission yields.

2.2 Models of Sub-Barrier Fusion

Sub-barrier fusion refers to fusion at incident energies below the Coulomb barrier, which is classically forbidden but occurs due to quantum mechanical tunneling. Interest in the sub-barrier fusion of light ions stemed from their importance in astrophysical studies. However in the past few decades sub-barrier fusion of light, medium and heavy nuclei has been an active field of research in low and medium energy research and it has displayed the richness of data. An interesting observation is the interplay of nuclear structure and dynamics, that is, the sub-barrier fusion cross sections were strongly affected by the structure of the colliding nuclei. There were many experimental observations which could not be explained by the models which had been proposed initially. Here we discuss some of the models which are frequently used in the analysis of the sub-barrier fusion data. The understanding of any model for fusion must start from the concept of the potential between the two colliding partners, the ion-ion potential, so a brief description of the ion-ion potential is given in the following section.

The Ion-Ion Potential

The total potential as seen by the two ions is the sum of the Coulomb and the nuclear potentials. Apart from this there is a centrifugal potential which also contributes to the total. A representative plot of $V_l(r)$ was shown in Fig. 1.1. It can be seen that the potential possesses an outer maximum (which we term the fusion barrier) at the radial separation where the long range Coulomb and short range nuclear forces just balance each other. At smaller radial separations there is an attractive pocket in the potential which serves to trap the nuclei long enough for fusion to occur. The centrifugal potential increases the barrier heights and slightly shifts the barrier locations; it may eventually fill in the attractive pocket and in general serves to terminate fusion at large impact parameters. The different potentials are discussed below.

1. Coulomb Potential

This is the repulsive potential existing between two charged spheres at any inter-nuclear separation r. The potential is calculated assuming the charges to be point charges and the distance r is taken as the distance between the mass centres. In such a case the Coulomb potential V_C is given by

$$V_C(r) = \frac{Z_p Z_t e^2}{r} \tag{2.1}$$

where Z_p and Z_t are the charges of the projectile and target. Corrections to the Coulomb potential due to the finite size of the charge distributions are applied when the separation is less than $r_c = R_p + R_t$ where $R_p = r_0 A_p^{1/3}$ fm with r_0=1.3 fm and similarly for R_t. In that case $V_C(r)$ given by

$$V_C(r) = \left(\frac{Z_p Z_t e^2}{2\ r_c}\right)\ (3\ -\frac{r^2}{r_c^2}) \tag{2.2}$$

The Coulomb potential defined above is often used in optical model calculations, however it is a poor approximation of the Coulomb potential of two heavy ions when r_c is calculated with r_0 values as large as 1.3 fm. Some improvement in this potential can be obtained by arbitrarily making r_0 much smaller. A refined form of potential has been suggested by Bondorf [1].

2. Nuclear Potential

The nucleus-nucleus potential which is originating from the two body nucleon-nucleon interaction comes into effect when the inter nuclear separation is less than the interaction radius. There are some macroscopic models and also some parameterised phenomenological models to calculate the nuclear potential.

Folding Potentials

One basic approach is the folding model. The "single folding potential" of Gross and Kalinowski [2, 3] was obtained by folding the nucleon density distribution of one

fragment with a standard optical model potential for nucleon scattering from the other fragment. The calculations neglect the saturating properties of nuclear forces and thus produces potentials which are too deep, especially at the small separation relevant to the fusion problem. This difficulty is avoided in the potentials which are derived from the liquid drop model. Krappe and Nix [4, 5] proposed a "double folding potential" which is obtained by folding a Yukawa type interaction into two homogeneous sharply bound matter distributions. More ambitious approaches based on the Thomas-Fermi method, have been followed in deriving the "proximity potential" of Randrup *et al.* [6]. It should be noted that all of these potentials make use of the sudden approximation which implies frozen density distribution.

Proximity Potential

The approach here is to calculate the attraction between two surfaces of arbitrary shape in the limit in which the radii of curvature are large compared to the range of the force and the thickness of the surface. Making use of the semi-empirical parameters [7], one finds the result

$$V_n(r) \;=\; 4\pi\gamma b\bar{R}\phi(\xi) \tag{2.3}$$

where ξ denotes the ratio $s/b = (r - R_t - R_p)/b$, b is the surface thickness having a value of 1 fm and s is the minimum distance between the surfaces. The surface energy coefficient $\gamma = 0.9517(1 - 1.7826\ I^2)$, where $I = \frac{(N-Z)}{A}$ and N, Z and A refer to the combined system of the two interacting nuclei. For spherical nuclei the reduced radius of curvature $\bar{R}$ is given by

$$\bar{R} = R_t R_p/(R_t + R_p)$$

The R_i (R_p and R_t) are calculated from the equivalent sharp surface radii R by the relations,

$$R \;=\; 1.28\ A_i^{1/3} \;-\; 0.76 \;+\; 0.8\ A_i^{-1/3} \tag{2.4}$$

and

$$R_i = R\left[1 - (\frac{b}{R}). \ldots\right] \tag{2.5}$$

This gives good agreement for the tail of the potential with empirical data from elastic scattering of spherical nuclei.

The nuclear potential of Eqn. 2.3 is a product of the universal function $\phi(\xi)$ and a geometrical factor. Using nuclear Thomas–Fermi approximation Blocki *et al.* [7] have parameterised this universal function as

$$\phi(\xi) = \begin{cases} -3.437\exp[-\frac{\xi}{0.75}], & \xi > 1.5 \\ -0.5(\xi - 2.54)^2 - 0.085(\xi - 2.54)^3, & \xi < 1.5 \end{cases} \tag{2.6}$$

The generalised liquid drop potential of Krappe-Nix-Sierk [4, 5] is similar to the proximity potential, and double folding a Yukawa exponential function over a sharp surface density distribution takes into account both a finite range and a surface diffuseness. The range and new values for the liquid drop constants were determined from a global analysis of fission barrier heights, nuclear masses and elastic scattering. The potential is of the form:

$$\phi(\xi) = \begin{cases} -D(F + s/a)(R/r)e^{-s/a}, & s \geq 0 \\ -V + Br/R + C(r/R)^2, & s < 0 \end{cases} \tag{2.7}$$

where the range constant $a = 0.68$ fm and $V = 100$ MeV

Empirical Potentials

In this approach information on the real potential deduced from analysis of many elastic scattering data sets is used to obtain a nuclear potential of the liquid drop form. This approach is based on the observation that elastic scattering angular distributions mainly determine the real part of the optical potential at a point slightly inside the distance of closest approach for a trajectory leading to the rainbow angle. Christensen and Winther [8] derived a potential from elastic scattering data using the fact that the real part of the optical potential deduced from the data is

well determined around the 'sensitivity' radius (which lies outside the maximum of the potential). They listed some sixty heavy ion systems with $Z_p = 5 - 10$ and $Z_pZ_t = 25 - 820$.

Akyüz and Winther [9] have proposed the following parameterisation based on an extensive analysis of data on elastic scattering of light and heavy ions.

$$\begin{aligned} &U^N(r) = -S_0\bar{R}\exp\{-\tfrac{r-R}{a}\}; \qquad S_0 = 65.4\ MeVfm^{-1} \\ &\tfrac{1}{a} = 1.16\left[1 + 0.48(A_p^{-1/3} + A_t^{-1/3})\right]fm^{-1} \\ &R_i = (1.20\ A_i^{1/3} - 0.35)fm \\ &R = R_p + R_t \\ &\bar{R} = R_pR_t/(R_p + R_t) \end{aligned} \tag{2.8}$$

The potential can be used only for values of r larger than the contact radius R i.e., the minimal distance r_{cr}, it can be used for $r > r_{cr} = (R_1 + R_2 + 1.2)$. For avoiding such a limitation in this potential, the Woods-Saxon [10] parameterisation of the ion–ion potential is used.

The Woods-Saxon parameterisation with the subsidiary condition of being compatible with the value of the maximum nuclear force predicted by the proximity model yields,

$$\begin{aligned} &V_n(r) = \tfrac{-V_0}{1+\exp[(r-R_0)/a]} \\ &V_0 = 16\pi\gamma\bar{R}a \\ &R_0 = R_p + R_t + 0.29 \\ &R = 1.233A^{1/3} - 0.98A^{-1/3} \\ &\bar{R} = R_pR_t/R_p + R_t \\ &\gamma = \gamma_o[1 - \kappa(N_p - Z_p)/A_p(N_t - Z_t)/A_t] \end{aligned} \tag{2.9}$$

where a=0.63 fm , $\gamma_o = 0.95$ MeV fm^{-2} and $\kappa = 1.8$

Several analyses of experimental data on elastic scattering and fusion excitation functions have shown that the above parameterisation of the ion-ion potential with minor adjustments of the constants involved provides an acceptable description of the data. The Wood-Saxon parameterisation of Akyüz-Winther potential is a compromise between the empirical potentials [8] determined from the elastic scattering of light ions, and the proximity potential [7] describing the interaction between very

heavy ions. The potentials discussed so far are for the case of spherical nuclei. In the case of deformed nuclei, the same potentials can be used with some modification.

3. Centrifugal Potential

The centrifugal potential is given by

$$V_{cent}(r) = \frac{\ell(\ell+1)}{2\mu r^2}\hbar^2 \tag{2.10}$$

where ℓ is the angular momentum and μ is the reduced mass of the colliding nuclei.

2.2.1 The Sharp Cutoff Model for Fusion (Classical Picture)

As was pointed out in the previous section, there is a potential barrier existing between the colliding nuclei as they approach each other. In the classical case, fusion is possible only when the projectile energy $E_p > V_B$ where V_B is the height of the Coulomb barrier. Consider an impact parameter for which the two nuclei at the distance of closest approach touch each other. For the corresponding angular momentum l_{gr}, all partial waves from 0 upto l_{gr} will fuse. For estimating the fusion cross section, assume that the target and projectile interact only in two ways, either elastically scatter or fuse to form a compound nucleus. For a given impact parameter 'b', the radial motion is governed by the effective potential

$$V_b(r) = V(r) + E\frac{b^2}{r^2} \tag{2.11}$$

There exists a trajectory for which the potential barrier coincides with the energy E, which is known as the grazing trajectory b_{gr} and the corresponding radial separation is the barrier radius R_B. For all impact parameters $b < b_{gr}$ the configuration will lead to fusion. Normally R_B is taken as the s-wave barrier radius and V_B as the s-wave barrier height. For the case of grazing collision, we can write

$$V_{B\ell} = V_B + E\frac{b_{gr}^2}{R_B^2} = E \tag{2.12}$$

i.e.,

$$b_{gr} = R_B\sqrt{1 - \frac{V_B}{E}} \tag{2.13}$$

Since all impact parameters up to b_{gr} will fuse, the fusion cross section can be taken to the area of a disc of radius b_{gr} *i.e.*

$$\sigma_{fus} = \pi b_{gr}^2 \tag{2.14}$$

Thus

$$\sigma_{fus} = \pi R_B^2 \left(1 - \frac{V_B}{E}\right) \tag{2.15}$$

The classical picture of fusion has its quantal counter part where total reaction cross section is identified as fusion, *i.e.*

$$\sigma_{fus}(E) = \frac{\pi}{k^2}\sum_{\ell=0}^{\infty}(2\ell+1)T_\ell \tag{2.16}$$

where T_ℓ is the transmission coefficient and k is the wave number.
In the sharp cut-off approximation,

$$T_\ell = \begin{cases} 1, & \ell < \ell_{gr} \\ 0, & \ell > l_{gr} \end{cases} \tag{2.17}$$

Hence the summation in Eqn. 2.16 will go only upto ℓ_{gr}. Changing the summation to integration we get

$$\sigma_{fus}(E) = \frac{\pi}{k^2}\ell_{gr}(\ell_{gr}+1) \tag{2.18}$$

Substituting for ℓ_{gr} from the grazing condition

$$V_{B\ell} = V_B + \frac{\ell_{gr}(\ell_{gr}+1)\hbar^2}{2\mu R_B^2} = E \tag{2.19}$$

and putting $k = p/\hbar$ we again get back the classical expression of 2.15.

2.2.2 One Dimensional Barrier Penetration Model (1D-BPM)

A comparison of the experimental fusion data with the classical fusion cross section reveals that at above barrier energies the simple classical expression (Eqn. 2.15)

can explain the data. But at below barrier energies the experimental cross section deviates from the classical prediction indicating that the classical representation of T_ℓ is no longer valid. This suggests that there is a need to introduce the concept of barrier penetration which is a quantum mechanical phenomenon where there is a finite probability for the particle to penetrate through the barrier if the energy is less than the barrier height.

For calculating the fusion cross section in the tunneling picture, consider the radial Schrödinger equation

$$d^2\psi_\ell/dr^2 + k_\ell^2(r)\psi_\ell(r) = 0 \tag{2.20}$$

where $k_\ell(r)$ denotes the local wave number

$$k_\ell^2(r) = \frac{2\mu}{\hbar^2}\left[E - V_\ell(r)\right] \tag{2.21}$$

and

$$V_\ell(r) = V_{\text{Coul}}(r) + V_{\text{nucl}}(r) + V_{\text{cent}}(r) \tag{2.22}$$

The fusion cross section is obtained by solving the Schrödinger equation, on the assumption that there are only ingoing waves in the region inside the barrier and there exists incident and reflected waves outside the barrier. Another way to obtain the cross sections for fusion is to calculate the transmission coefficients for the passage either over or through the outer maximum in the interaction potential using the WKB method. Specifically, the transmission coefficients T_ℓ are related to partial cross section as

$$\sigma_\ell(E) = \pi\lambda\!\!\!^{-2}(2\ell+1)T_\ell(E) \tag{2.23}$$

The relationship between the action integral and the transmission coefficient $T_\ell(E)$ is given by

$$T_\ell(E) = [1 + \exp(-2K_\ell(E))]^{-1} \tag{2.24}$$

and

$$K_\ell(E) = \pm\int_{r_a}^{r_b}\sqrt{\frac{2\mu}{\hbar^2}\left(V_\ell(r) - E\right)}dr \tag{2.25}$$

where r_a and r_b denote the outer and inner turning points of the barrier and minus/plus signs in front of the integral pertains to above/below barrier energies. Calculating $T_\ell(E)$ in this form is possible only through numerical integration. An analytical form for T_ℓ has been given by Hill-Wheeler [11] where the barrier is taken to be nearly parabolic and is replaced by an inverted harmonic oscillator potential, *i.e.*

$$\begin{aligned} V_\ell(r) &= V_B - \frac{1}{2}m\omega_o^2\,(r-R_B)^2 + \frac{\hbar^2\ell(\ell+1)}{2\mu r^2} \\ &= V_{B\ell} - \frac{1}{2}m\omega_o^2\,(r-R_B)^2 \end{aligned} \tag{2.26}$$

Simplifying, we get

$$T_l = \left[1+\exp\frac{2\pi}{\hbar\omega}\,(V_{B\ell} - E)\right]^{-1} \tag{2.27}$$

where $V_{B\ell}$ denotes the barrier height for the ℓ-th partial wave and $\hbar\omega_\ell$ is the corresponding barrier curvature. Hence the fusion cross section σ_ℓ can be written as

$$\begin{aligned} \sigma_l &= \pi\lambda\!\!\!^{-2}\,(2l+1)\;T_l \\ &= \pi\lambda\!\!\!^{-2}\,(2l+1)\left[\,1+\exp\frac{2\pi}{\hbar\omega_l}(V_{Bl}-E)\right]^{-1} \end{aligned} \tag{2.28}$$

Making the further approximations that,

$$\hbar\omega_\ell \approx \hbar\omega_0 \quad ; \quad V_{B\ell} = V_B + \hbar^2\ell(\ell+1)/2\mu R_B^2$$

one obtains the total fusion cross section as

$$\begin{aligned} \sigma_{fus} &= \sum_l \sigma_\ell \\ &= \pi\lambda\!\!\!^{-2}\sum_{l=0}^{\infty}(2l+1)\left[1+\exp\frac{2\pi}{\hbar\omega_0}(V_B - E + \frac{l(l+1)\hbar^2}{2\mu R_B^2})\right]^{-1} \end{aligned} \tag{2.29}$$

replacing the summation by integration [12] one gets,

$$\begin{aligned} \sigma_{fus} &= \int_0^\infty \sigma_l \\ &= \pi\lambda\!\!\!^{-2}\int_0^\infty(2l+1)\left[1+\exp\frac{2\pi}{\hbar\omega_0}(V_B - E + \frac{l(l+1)\hbar^2}{2\mu R_B^2})\right]^{-1} \end{aligned} \tag{2.30}$$

which gives the Wong's formula for fusion cross section

$$\sigma_{fus} = \frac{R_B^2 \hbar\omega_0}{2E} ln\{1 + \exp[\frac{2\pi}{\hbar\omega_0}(E - V_B)]\} \tag{2.31}$$

For energies $E >> V_B$ the above equation reduces to the classical expression for fusion cross section

$$\sigma_{fus} = \pi R_B^2 [1 - \frac{V_B}{E}] \tag{2.32}$$

and for sub barrier energies, ie $E << V_B$ we get

$$\sigma_{fus} = \frac{R_B^2 \hbar\omega_0}{2E} \exp\{\frac{2\pi}{\hbar\omega_0}(E - V_B)\} \tag{2.33}$$

The fusion cross section, σ_{fus} shows a linear dependence with 1/E at above barrier energies (Eqn. 2.32). As the energy is decreased there are departures from this linearity and in particular Eqn. 2.33 shows that σ_{fus} increases exponentially with $(E - V_B)$.

Failure of the 1D-BPM - We have so far assumed that fusion, that is absorption occurs in the elastic channel only. In this case, the only dynamical variable in the problem is the distance between the two fusing nuclei, for which reason this is called the one-dimensional barrier penetration model (1D-BPM). The 1D-BPM is adequate to describe the fusion of light systems. However this is no longer true for heavier systems. The reason for this failure is that an increasing number of non elastic channels have to be taken into account for heavier systems, giving rise to a behaviour of fusion cross section which cannot be reproduced by the one dimensional model (see Fig. 1.5).

As the two fusing nuclei approach each other, they will in general undergo transitions from the ground state to the excited states and transfer particles between themselves, before going close enough to form a compound nucleus. The elastic channel couples to non elastic channels and the transmission across the barrier takes place in each of these channels as well. The incoming wave splits up into various

inelastic waves with transmission probabilities T_n, which have to be combined in order to obtain the total transmission probability into the interior of the compound system. Since the channel energy in the non elastic channel is lower than in the elastic channels, implying smaller transmission coefficient one expects to find a lower total transmission for the coupled case. On the other hand the interactions which are responsible for the coupling also contribute to the effective barrier in the various channels with the net effect of lowering them. This would lead to an enhancement of the transmission coefficient. This is the basis of the coupled channels formalism [13] for fusion which will be discussed in detail in the next chapter.

2.2.3 Geometric Models

Static Deformation

In a large number of nuclei the low lying states are dominated by collective excitations of rotational character. For these nuclei the coupling of the relative motion to the rotational states may be described in the corresponding classical limit, as the fusion of two rigid rotors [14, 12]. If the excitation energy is small, then the time scale of the rotation is slow in comparison to the relative motion and the nuclei may be assumed to be frozen in shape and orientation during the interaction. The fusion cross section in that case depends on the mutual orientation of the nuclei as

$$\sigma_{fus}(E) = \frac{1}{16\pi^2} \int \sigma_f(E, \theta_1, \theta_2) d\Omega_1 d\Omega_2 \tag{2.34}$$

where $\sigma_{fus}(E, \theta_1, \theta_2)$ is the differential cross section for a particular mutual orientation defined by angles θ_1 and θ_2, and the $d\Omega_i$ are solid angle elements. The $\sigma_{fus}(E, \theta_1, \theta_2)$ are calculated by expanding the nuclear shapes in terms of spherical harmonics which yield a specific fusion radius for each orientation. This approach has been applied to the fusion of ^{16}O with the series of even-A (A = 144 - 154) Samarium isotopes [15]. These isotopes undergo a shape transition with increasing neutron number from spherical to prolate deformed. This is manifested as more cross section at sub-barrier energies for the deformed target. While the geometric

model explains the trend of this isotopic change in fusion enhancement correctly, it overestimates the cross sections in many cases. This is presumably due to the neglect of the excitation energies that is the frozen approximation.

Quantal Zero-Point Motion

In a collective model of surface vibrations the nuclear radius is parameterised in terms of the vibrational amplitudes $a_{\lambda\mu}$ as

$$R(\theta) = R_0(1 + \Sigma_{\lambda\mu} a_{\lambda\mu} Y^*_{\lambda\mu}(\theta)) \tag{2.35}$$

where R_0 denotes the equilibrium radius. In the limit of small oscillations the energy becomes a quadratic function of the amplitudes and their time derivatives. The equation of motion is

$$\ddot{\alpha}_{\lambda\mu} + \omega^2_\lambda \alpha_{\lambda\mu} = 0 \tag{2.36}$$

where the amplitudes $\alpha_{\lambda\mu}$ undergo harmonic oscillations with frequency ω_λ. In the work of Esbensen [16] the vibrational amplitudes were interpreted as representing zero-point fluctuations. Assuming that the amplitudes $\alpha_{\lambda\mu}$ are completely independent, their ground state distributions are uncorrelated Gaussians. This, in turn, implies that the distribution of nuclear radii about the equilibrium value R_0 is obtained by folding these various Gaussians. As a result, it too is a Gaussian. The Gaussian distribution of radii plays the same role in zero-point motion as does the angle averaging in the static deformation approach. Esbensen showed that quantal zero-point motion can account for the observed behaviour of the cross sections of sub-barrier fusion of $^{16}O + {}^{148-154}Sm$. In general, his approach represents an extension of the geometric approach to vibrational nuclei. As was the case for static deformations, the non-zero excitation energy of the coupled state or states is neglected. This model also tends to over predict the cross sections for fusion of massive nuclei.

2.2.4 Energy Dependent Barrier Penetration Model

It has been shown earlier that coupling of the entrance channel to various inelastic and transfer channels contributes appreciably to the sub-barrier enhancement and the accompanying broadening of the spin distribution. However, a theoretical description of the fusion process in terms of the coupled channels formalism becomes quite involved and often impractical when there are a large number of contributing channels. An additional deficiency of the coupled channels approach is the way in which fusion is treated in these calculations, where the dynamical effects are all shielded. It has been shown that by using a suitable energy dependence of the fusion barrier height, it may still be possible to explain the data by the one dimensional barrier penetration picture. Evidence for energy dependent interaction potentials has also come from measurements of heavy ion elastic scattering cross sections close to the Coulomb barrier (threshold anomaly) and the energy dependence is believed to arise due to the coupling of elastic channel to other non elastic channels. However Dasso, Landowne and Pollarolo [17] showed that such a model is inconsistent as it fails to reproduce the calculated energy dependence of the compound nucleus spin distributions. Later Mohanty *et al.* [18, 19] showed that the results of a model coupled channels calculation can be reproduced by a simple barrier penetration model with energy dependent barriers, where the barrier heights are treated as a function of the effective radial kinetic energy rather than the centre of mass bombarding energy.

2.2.5 Stelson Model

Stelson proposed a model to explain the observed enhancement of the sub-barrier fusion cross sections. According to Stelson [20, 21], if one assumes a flat distribution of barriers D(B), symmetric about a mean barrier B and having a sharp cut off at T, where T is the threshold barrier, then the expression for fusion cross section at

near barrier energies takes the form

$$\sigma_{fus} = \pi R_B^2 \frac{(E-T)^2}{4E(B-T)} \tag{2.37}$$

where the distribution is assumed to be

$$D(B) = \begin{cases} [2(B-T)]^{-1} & \text{for} \quad T \leq E \leq (2B-T) \\ 0 & \text{elsewhere} \end{cases} \tag{2.38}$$

The parameters R_B, B, T are varied to get a best fit to the measured excitation function. From these analysis, it was seen that the inter nuclear separation distance is larger for the threshold barrier T than the separation for the mean barrier B *i.e* there exists a mechanism that is strong enough to overcome the Coulomb force at large distances and produce fusion. The threshold barrier T is determined by the barrier at a distance of approach at which the least bound neutron may flow from one nucleus to another. Based on these arguments, Stelson proposed that as the colliding nuclei approach each other and the nuclear surface start overlapping, a stage is reached when the barrier for neutron flow across the nuclei vanishes. Thus neutron flow triggers the fusion process at distances typically 1 - 2 fm larger than the mean barrier distance.

2.2.6 The Neck Formation Model

The idea that flow of neutrons between the colliding nuclei may precede and initiate fusion has encouraged the development of the neck formation model. In this model [22, 23] the nuclei are treated as macroscopic spheroids on a potential energy surface which depends on the inter-nuclear separation and the deformation of the nuclei. It is assumed that the deformation in the direction of the relative motion, which eventually leads to the formation of a neck between the reactants is the most important degree of freedom of the nuclear binary system apart from the relative motion itself. The fusion mechanism is found to be dominated by two characteristics of the neck formation process:

1. the disappearance of the potential barrier along the neck degree of freedom when the nuclei reach a critical radial separation R_n;

2. the very small values of the mass tensor element associated to the neck variable in the early stages of the collision.

Owing to these effects the system becomes unstable with respect to neck formation at separations $r \leq R_n$. Since R_n is larger than the radius R_B of the Coulomb barrier, this instability appears at a collision energy E = $V_n < V_B$, where V_n and V_B are the values of the total potential (Coulomb + nuclear) at the radial separation R_n and R_B, respectively. The consideration of a neck degree of freedom leads, therefore to an effective barrier lowering

$$\Delta B = V_B - V_n$$

It was shown that at very low energies the fusion cross section predicted by the neck formation model is very close to that calculated with the one-dimensional model at an energy E + ΔB. The enhancement of the fusion cross section arising from neck formation leads, therefore to an asymptotic energy shift $\Delta E \approx \Delta B$.

2.2.7 The Optical Model for Fusion

Any coupled channels problem can, in principle, be reduced to an effective one-channel optical potential, $U(E) = V(E) + iW(E)$ which describes the elastic scattering, while the expectation value of W gives the reaction cross section. W can be decomposed as $W(E) = W_f(E) + W_d(E)$, where the expectation value of W_f gives the fusion cross section and that of W_d gives the cross section for quasi-elastic or direct reactions. This is the formal basis of the optical model of Udagawa *et al.* [24]. If W_f is confined inside the Coulomb barrier and the peripheral damping due to W_d is neglected this model is equivalent to the original one-channel barrier penetration model except that the real potential V(E) and hence the barrier height is allowed to be E-dependent. However it then does not give broad enough spin

distributions. The optical model of Udagawa goes beyond this by allowing W_f to extend to larger radii, into the barrier itself and this gives broader $\sigma_{fus}(\ell)$. Once we relax the constraint of confining W_f to smaller radii, a variety of $\sigma_{fus}(\ell)$ shapes and larger values of $< \ell^n >$ may be obtained.

A plausible interpretation of a large radial extent for W_f is that it is due to the multi-step contributions to fusion that are described explicitly in the coupled channels calculations. Formally, W_f itself may be decomposed, $W_f(E) = W_{of}(E) + W_{pf}(E)$ where W_{of} is the "bare" fusion absorptive potential to be used in the coupled channels calculations and W_{pf} is the additional "polarisation" term that arises when the coupled channel equations are projected onto the elastic channel. Thus W_{pf} accounts for fusion that occurs after non elastic transitions into various direct channels, transfer or inelastic. This would be expected to be more peripheral than W_{of}, especially at sub-barrier energies, so that W_f in an optical model description could extend into or even beyond the barrier even if the bare W_{of} were confined inside.

In summary, there exists several models of fusion which qualitatively account for the fusion enhancement. However many of these models lack the quantitative details to simultaneously predict the excitation function, spin distribution and barrier distribution. A unique model taking into account all the dynamical features of fusion is yet to emerge.

Bibliography

[1] J. P. Bondorf, M. J. Sobel and D. Sperber, Phys. Rep. **15c**, 83 (1974).

[2] D. H. E. Gross, H. Kalinowski, Phys. Lett. **48B**, 302 (1974).

[3] D. H. E. Gross, H. Kalinowski, J. N. De, **HE 74** p 174.

[4] H. J. Krappe, J. R. Nix and A. J. Sierk, Phys. Rev. Lett. **42**, 215 (1979).

[5] H. J. Krappe, J. R. Nix and A. J. Sierk, Phys. Rev. **C20**, 992 (1979).

[6] J. Randrup, W. J. Swiatecki, C. F. Tsang, Lawrence Berkeley Laboratory Report No. 3603 (1974)

[7] J. Blocki, J. Randrup, W. J. Swiatecki, and C. F. Tsang, Ann. Phys. (N.Y.) **105**, 427 (1977).

[8] P. R. Christensen and A. Winther, Phys. Lett. **65B**, 19 (1976).

[9] O. Akyüz and A. Winther, Proceedings of the Enrico Fermi International School of Physics, 492 (1979), edited by R. A. Broglia, C. H. Dasso, and R. Ricci, North – Holland, Amsterdam, 1981.

[10] R. A. Broglia and A. Winther, Heavy ion Reactions, Vol I (1981), The Benjamin /Cummins Pub. Co. Inc.

[11] D. L. Hill and J. A. Wheeler, Phys. Rev. **89**, 1102 (1953).

[12] C. Y. Wong, Phys. Rev. Lett. **31**, 766 (1973).

[13] C. H. Dasso, S. Landowne and A. Winther, Nucl. Phys. **A405**, 381 (1983); C. H. Dasso, S. Landowne and A. Winther, Nucl. Phys. **A407**, 221 (1983).

[14] J. O. Rasmussen, K. Sugawara-Tanabe, Nucl. Phys. **A171**, 497 (1971).

[15] R. G. Stokstad, E. E. Gross, Phys. Rev. **C23**, 281 (1981).

[16] H. Esbensen, Nucl. Phys. **A352**, 147 (1981).

[17] C. H. Dasso, S. Landowne, G. Pollarolo, Phys. Lett. **B133**, 217 (1989).

[18] A. K. Mohanty, S. V. S. Shastry, S. K. Kataria, V. S. Ramamurthy, Phys. Rev. Lett. **65**, 1096 (1990).

[19] A. K. Mohanty, S. V. S. Shastry, S. K. Kataria, V. S. Ramamurthy, Phys. Rev. **C46**, 2012 (1992).

[20] P. H. Stelson, Phys. Lett. **B205**, 190 (1988).

[21] P. H. Stelson, H. J. Kim, M. Beckerman, D. Shapira R. L. Robinson, Phys. Rev. **C41**, 1584 (1990).

[22] C. E. Aguiar, A. N. Aleixo, V. C. Barbosa, L. F. Canto, R. Donangelo, Nucl. Phys. **A500**, 195 (1989).

[23] C. E. Aguiar, V. C. Barbosa, L. F. Canto, R. Donangelo, Nucl. Phys. **A472**, 571 (1987).

[24] T. Udagawa et al., Phys. Rev. **C32**, 124 (1985); Phys. Rev. **32**, 1435 (1985).